

**Proceedings of the ASME 2024  
International Design Engineering Technical Conferences & Computers and  
Information in Engineering Conference  
IDETC2024  
AUGUST 11-14, 2024, Washington DC, USA**

**IDETC2024-141907**

**CONSTRUCTION OF 3D ENGINEERED GLIOMA TISSUES**

**USING ACOUSTIC PATTERNING DEVICE**

<b>Yingshan Du</b> Virginia Tech Blacksburg, VA, 24060	<b>Jiali Li</b> Virginia Tech Blacksburg, VA, 24060	<b>Liang Shen</b> Virginia Tech Blacksburg, VA, 24060	<b>Zhe Pei</b> Virginia Tech Blacksburg, VA, 24060
<b>Bowen Cai</b> Virginia Tech Blacksburg, VA, 24060	<b>Teng Li</b> Virginia Tech Blacksburg, VA, 24060	<b>Chongpeng Qiu</b> Virginia Tech Blacksburg, VA, 24060	<b>Zhenhua Tian</b> Virginia Tech Blacksburg, VA, 24060 <a href="mailto:tianz@vt.edu">tianz@vt.edu</a>

**ABSTRACT**

Cell patterning techniques play a pivotal role in the development of three-dimensional (3D) engineered tissues, holding significant promise in regenerative medicine, drug screening, and disease research. Current techniques encompass various mechanisms, such as nanoscale topographic patterning, mechanical loading, chemical coating, 3D inkjet printing, electromagnetic fields, and acoustic waves. In this study, we introduce a unique standing bulk waves-based acoustic cell patterning device designed for constructing anisotropic engineered glioma tissues containing acoustically patterned human glioblastoma cell U251. Our device features two orthogonal pairs of piezoelectric transducers securely mounted on a customized holder. The energy of standing bulk waves generated from these transducers can transmit into the medium in a Petri dish through its bottom wall. Cells

in the medium can be directed to the local minima of Gor'kov potential fields and trapped by the resultant acoustic radiation force. Through proof-of-concept experiments, we validate the functionality of our acoustic patterning device and assess the morphology and differentiation of U251 cells within the engineered glioma tissues. Our findings reveal that cells can be arranged in different distributions, such as parallel-line-like and lattice-like patterns. Moreover, the aligned cells exhibit more obvious elongation along the cell alignment orientation compared to the result of a control group. We anticipate that this study will catalyze the advancement in contactless cell patterning technologies within tissue engineering, facilitating the development of engineered tissues for applications in regenerative medicine and disease research.

**Keywords:** Acoustic patterning, tissue engineering, cell patterning, standing acoustic waves, acoustic tweezers

## 1 INTRODUCTION

Engineered tissues[1] have garnered significant attention for various applications within the realms of regenerative medicine,[2,3] drug screening,[4,5] and disease modeling.[6,7] An ultimate goal of three-dimensional (3D) engineered tissues is to emulate the cellular activities found in natural tissues and replicate the functional histoarchitecture of living tissues and organs. In the context of natural *in vivo* tumors, such as malignant gliomas, the arrangement of cells becomes oriented, a phenomenon distinct from benign states because of cell migration.[8] However, a key challenge to the construction of engineered tissues with biomimetic features is the precise arrangement of seed cells to construct anisotropic biomimetic tissues.

Numerous interdisciplinary methods have been developed to achieve different cellular arrangements in 3D engineered tissues. These methods leverage different mechanisms such as nanoscale topographic patterning, [9,10] mechanical loading,[11] chemical coating,[12] 3D printing,[13] and electromagnetic fields.[14],[15] Recent advancements in acoustic cell patterning methods have shown promise in aligning neurons,[16],[17] muscle bundles,[18] and cardiac myocytes.[19],[20] This approach not only promotes significant tensile anisotropy but also offers a novel platform for achieving anisotropic tissue morphologies[21].

Here, we introduce a standing bulk acoustic waves (BAW)-based device capable of sending acoustic waves into a cell medium loaded in a Petri dish and further arranging cells using acoustic radiation forces without direct physical contact with the medium and cells. This BAW device utilize piezoelectric transducers to convert electrical excitation signals into mechanical waves. [22] Counter-direction acoustic waves generated by a pair of transducers interact with each other, further generating standing acoustic waves, which have spatially periodic pressure distribution in the liquid medium. The number of pressure nodes and antinodes generated in the domain of interest can be customized by adjusting the wave frequency. In a standing acoustic field, the acoustic radiation forces applied on cells highly affect the moving trajectory of cells and the distribution of cells at force equilibrium states. Through acoustic manipulation, cells can be precisely trapped at the pressure nodes of standing waves.[23]

In our study, we designed and manufactured an in-Petri dish acoustic cell patterning device and then utilized this device to aggregate glioma cells in a 3D environment, facilitating closer growth and providing patterned 3D engineered glioma tissues. Additionally, we conducted microscopic characterization to evaluate the morphology of engineered tissues with patterned cells, as well as cell differentiation. Our experimental

study demonstrates the capability of our acoustic patterning device for aggregating and patterning glioma cells in a 3D culturing environment, thereby facilitating the development of engineered glioma tissues with interconnected networks.

## 2 METHODS

### 2.1 Acoustic cell patterning device

Figure 1 depicts a BAW-based standing wave device designed for cell patterning. The device utilizes two orthogonal pairs of piezoelectric transducers (PZTs) with dimensions of  $20 \times 15\text{c} \times 2.1\text{mm}$  (STEINER & MARTINS, INC.) and resonance frequencies of 3.20, 5.44, and 7.50 MHz. A customized 3D fixture, designed to support the vertically inserted PZTs, is positioned within deionized (DI) water. A glass-bottom Petri dish (Nest, 35 mm diameter) is then inserted into the assembled device. Beneath the glass-bottom Petri dish, there is a thin layer of DI water that is considered as a coupling medium for transmitting acoustic waves generated by the PZTs into the Petri dish. To excite the two pairs of transducers for generating standing acoustic waves, continuous sinusoidal signals at transducer resonance frequencies are generated by a function generator (Tektronix, AFG3022C). The generated signals are amplified using a power amplifier (E&I, model A150) before being applied to the transducers. The entire acoustic cell patterning process is completed within 5 minutes.

As depicted in Figure 1, the acoustic patterning device is specifically designed for patterning cells in Petri dishes. Its unique feature lies in its ability to arrange suspended cells loaded in a Petri dishes, a common biomedical lab supply, making it an easy-to-use tool for cell arrangement with minimized contamination.

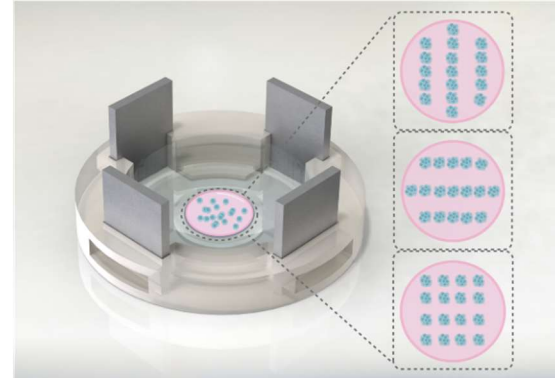


**FIGURE 1:** Schematic of the in-Petri dish acoustic patterning device, which has two orthogonal pairs of PZTs to arrange cells in a Petri dish into different patterns.

### 2.2 Cell and tissue culture

The human glioblastoma cell line, U251 cells, was sourced from the Biomedical Engineering

Department (Virginia Tech). Before experiments, U251 cells were cultured in Dulbecco's Modified Eagle's Medium supplemented with High Glucose and L-Glutamine, (DMEM; GenClone, USA), 10% fetal bovine serum (FBS), and 1% Penicillin-Streptomycin (GenClone, USA), and maintained at 37°C in a 5% CO<sub>2</sub> incubator. Passaging was conducted twice weekly using 0.05% trypsin-EDTA (sc-363354, Santa Cruz Biotechnology, Inc.), followed by resuspension in culture medium. The adhesive culture method was employed for U251 cell culture.

A collagen solution was utilized to construct the cell scaffold due to its excellent cytocompatibility and biodegradability. To prepare a collagen solution containing cells, initially, the pH of a 200 $\mu$ L 5mg/mL collagen stock solution was adjusted by adding 15 $\mu$ L of 0.1 N NaOH. Subsequently, it was added into the collagen solution that a mixture of 1 $\times$ 10<sup>6</sup> cells/mL 150 $\mu$ L cell suspension and 35 $\mu$ L 10 $\times$  PBS was prepared to maintain a final concentration of 2.5mg/mL and pH in the range of 7.2-7.4. After gelation of the collagen solution, an engineered collagen hydrogel construct containing U251 cells were cultured in a culture medium for 7 days, with the culture medium being replaced every three days.

### 2.3 Construct a glioma tissue with acoustically patterned U251 cells

The collagen solution containing cells was kept on ice to prevent pre-crosslinking of the collagen and then transferred into a glass-bottom Petri dish, which was then placed at the center of the acoustic device. Prior to cell patterning, the deionized water (*i.e.*, a coupling layer between acoustic transducers and the Petri dish) was also cooled to a low temperature for prevent pre-crosslinking of the collagen before tuning on acoustic waves. The excitation frequency of the PZTs was adjusted to their respective working frequencies, such as 3.20, 5.44, and 7.50MHz. An excitation amplitude of 20 Vpp was set for trapping cells at the acoustic pressure nodes within the cell suspension. Cell patterns were constructed and further kept in the acoustic field for 5 minutes during the collagen gelation, which was triggered by the slight temperature increase induced by acoustic waves. Subsequently, the Petri dish with the constructed cell patterns was transferred to a 37°C incubator to further facilitate collagen gelation. The control tests with randomly distributed cells were performed using an identical protocol but without acoustic patterning.

### 2.4 Immunofluorescent staining

Engineered glioma tissues were washed in 1 $\times$  PBS to remove the culture medium and then fixed with 4% paraformaldehyde (Sigma) for 10 minutes at room temperature. Following fixation, all tissue samples

were blocked and permeabilized using a 5% bovine serum albumin (BSA) solution and 0.1% Triton X-100 for 30 minutes at room temperature. Subsequently, the samples were incubated with a polyclonal GFAP fluorescent antibody (1:100, Bio Legend) overnight at 4°C. On the following day, the samples were rinsed twice with 1 $\times$  PBS and then counterstained with DAPI before observation.

### 2.5 Image analysis

Engineered glioma tissues were imaged using a confocal laser scanning microscope (Zeiss, LSM 800) equipped with 5 $\times$  and 10 $\times$  objectives. GFAP Alexa 488 fluorescence was excited using an Argon laser at 488 nm, while DAPI fluorescence was excited using a UV laser at 350 nm.

All experiments were conducted independently and repeated at least three times to ensure reproducibility. Additionally, each experimental group consisted of at least six samples to provide statistically meaningful results.

### 2.6 Analytical simulations

To predict the acoustic pressure, intensity, and radiation force fields generated by one parallel pair and two orthogonal pairs of PZTs, we developed an analytical model. Figure 2 shows the schematics of cases with different transducers turned on. The codes were written based on the MATLAB language.

## 3 RESULTS

### 3.1 BAW-based device mechanism

Figure 1 depicts a schematic of the standing BAW-based in-Petri dish cell patterning device and illustrates the different patterns (such as parallel-like-line and lattice-like patterns) that can be generated by our device. This device generates acoustic waves that are converted into elastic waves in Petri dish's glass bottom. Subsequently, the wave energy leaks into the cell medium in the Petri dish to form standing acoustic waves. These standing waves create Gor'kov potential wells, typically located at pressure nodes, acting as virtual, non-contact acoustic tweezers trapping cells for patterning. As shown by simulation results in Figure 2j, 2k, and 2l, the device can generate acoustic radiation forces having directions towards acoustic pressure nodes.

Figures 2g-2i display various cell patterns achieved by the acoustic patterning device, when different pairs of PZTs are excited. One parallel pair of PZTs, either a horizontal or vertical pair of PZTs, can produce different parallel-line-like acoustic patterns (Figures 2d and 2e), while the activation of two orthogonal pairs of PZTs results in a dot matrix-like acoustic pattern (Figure 2f). The bright field image (Figure 2i) reveals cells assembled in multiple

clusters within the acoustic potential wells, forming the dot pattern. Figures 2g and 2h demonstrate the alignment of cell cells along pressure node lines.

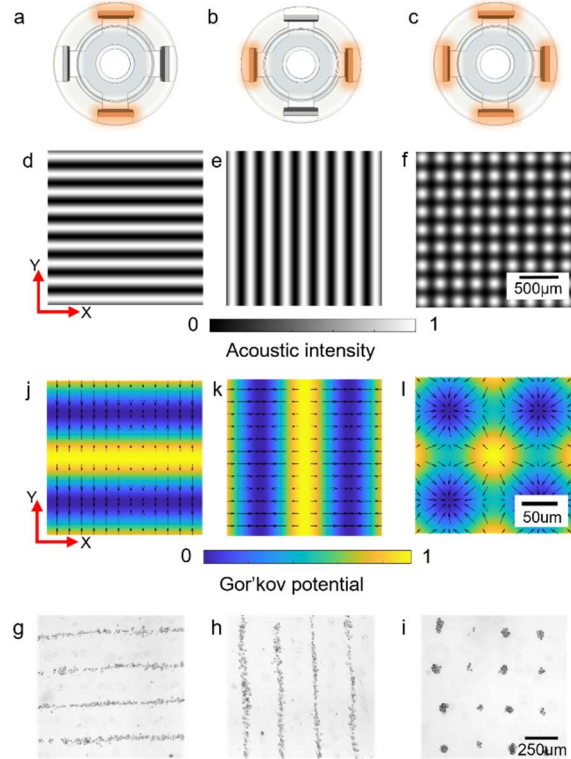


**FIGURE 2:** Schematics and results of using our acoustic device for cell patterning. (a-c) Schematics showing the locations of the excited PZTs. (d-f) Simulated acoustic intensity fields when using different PZTs (high intensity, red; low intensity, black). The scale bar is 500μm. (j-l) Simulated acoustic radiation force fields (arrows). The scale bar is 50μm. (g-i) Brightfield microscopic images showing different cell patterns. The scale bar is 250μm.

### 3.2 Constructing different patterns of U251 cells at different acoustic frequencies

At different operation conditions such as different frequencies and different pairs of transducers, our device can generate different cell patterns. Figure 3 given obtained cell patterns at different conditions. First, we excited the horizontal pair of PZTs at three different frequencies: 3.20, 5.44, and 7.50 MHz. Figures 3a-3c show parallel-line-like cells patterns constructed as those three frequencies, and they show the change in the spacing between cell lines at different excited frequencies. Additionally, a dot matrix-like cell pattern was constructed, when the two orthogonal pairs of PZTs were excited at different frequencies. Figure 3d, for example, depicts a rectangular dot matrix pattern achieved at the excitation frequency combination of  $3.20 \times 5.44$  MHz, compared to the square dot matrix pattern shown in Figure 2i.

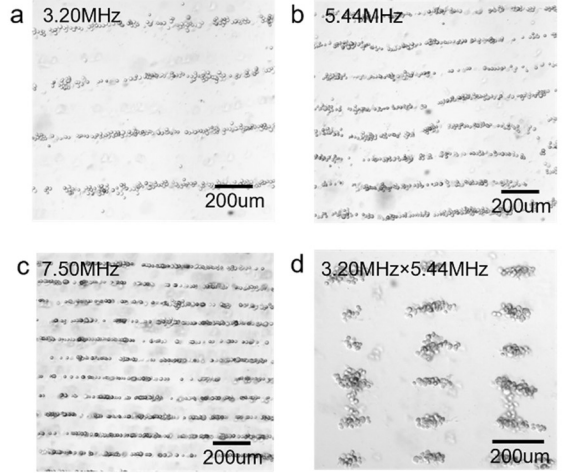


**FIGURE 3:** Captured brightfield images showing constructed cell patterns when using at different acoustic frequencies. The excited frequencies contain (a) 3.20MHz; (b) 5.44MHz; (c) 7.50MHz; (d) 3.20MHz  $\times$  5.44MHz.

### 3.3 U251 cell patterns in collagen hydrogel constructs

Our primary objective is the construction of developed glioma tissues, necessitating the observation of U251 cell differentiation within the engineered tissues. Utilizing 2.5 mg/mL collagen with a single horizontal pair of PZTs at a frequency of 3.20 MHz, we conducted experiments to arrange cells and then assess the differentiation of cells. Figure 4 presents the bright field images of patterned (test group) and randomly distributed cells (control group) in different collagen hydrogel constructs. On day 0, random distributions of cells were observed in the control groups (Fig. 4a), while cells in the experimental groups were aligned and aggregated by acoustic pressure nodes, forming parallel lines (Fig. 4c). After three days of culture, cells experienced differentiation and extended their lengths (Fig. 4b and 4d). In the control groups, cells remained in a random distribution and extended in various directions (Fig. 4b). Conversely, in the experimental groups, cells predominantly aligned along the lines, exhibit increased lengths along the alignment direction. The closer proximity of cells within the lines facilitated cellular communication.

To verify cellular connection and differentiation in the engineered glioma tissues, Figure 5 presents fluorescent images for both control and experimental groups on Day 3. Immunostaining revealed widespread expression of GFAP, indicating differentiation of U251 cells into glial cells. Notably, the control groups exhibited a more random organization, whereas experimental groups displayed organized and highly aligned cell networks. Our results also demonstrate the ability to establish

connections between cell lines after acoustic patterning, with cells forming long bundles by Day 3. Consequently, effective intercellular connections are increased in patterned samples.

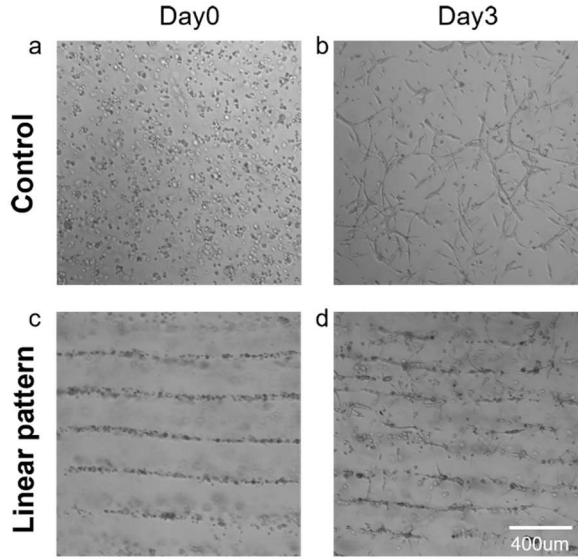


**FIGURE 4:** The bright field results of cell morphology in unpatterned and patterned groups. (a, b) Results of unpatterned cells on days 0 and 3. (c, d) Results of patterned cells on days 0 and 3.

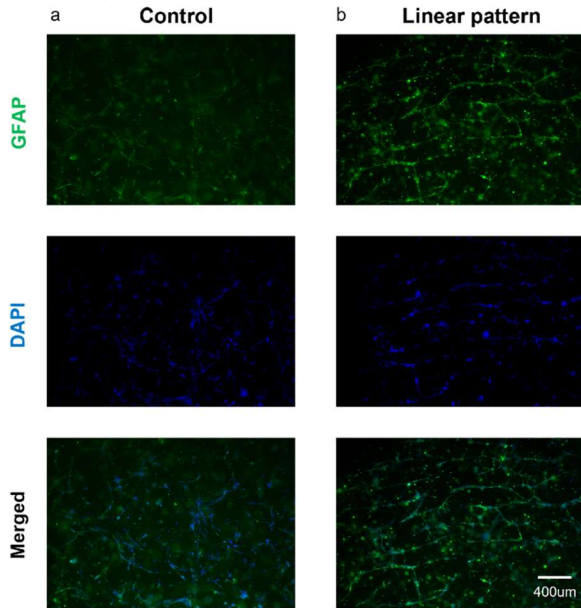


**FIGURE 5:** Confocal fluorescence microscopy images showing the unpatterned and patterned groups on day 3. (a) Results of unpatterned groups. (b) Results of patterned groups. (Green, GFAP; Blue, DAPI)

#### 4 DISCUSSION AND CONCLUSION

In this study, we built and validated an acoustic patterning device for constructing 3D engineered glioma tissues. The device comprises two orthogonal pairs of piezoelectric transducers positioned around a

glass-bottom Petri dish. These transducers generate standing BAWs within the fluid layer under the glass-bottom Petri dish, and the wave energy can further transmit into the cell medium in the Petri dish for patterning cells. This acoustic approach is easy-to-use and minimized direct contact with cells and the medium to ensure low cross contamination during cell patterning. Our experimental findings demonstrate that U251 cells can be effectively patterned within a viscous collagen solution using our acoustic patterning device. When compared with samples having unpatterned cells, the constructed glioma tissues with patterned cells exhibited a closer cellular arrangement, with cells displaying extended lengths along the cell alignment direction. This arrangement with controlled intercellular distances can foster stronger intercellular connections, facilitating cellular communication, as well as the passage of chemical or electrical signals between interacting cells.

Of particular note, our device transmits energy indirectly to cell clusters through the water layer serving as an ultrasound coupling layer, rather than directly placing transducers in the cell medium. As a result, our device operates more gently and minimizes possible contamination. Moreover, our acoustic platform enables cell patterning in Petri dishes without the need to place transducers within the dish, thereby reducing the risk of cross-contamination between different tests. Unlike other patterning methods such as nanoscale topographic patterning, acoustic patterning offers dynamic reconfigurable cell patterns. Furthermore, the distribution of the acoustic wells can be adjusted by varying the input powers and frequencies for the used piezoelectric transducers.

Our acoustic patterning device is user-friendly and easy-to-fabricate. Its excellent biocompatibility and the ability to accommodate different sample sizes allow for the manipulation of single cells, cell clusters, and cell spheres. We anticipate that our acoustic patterning device will serve as a valuable tool in tissue engineering, particularly in utilizing engineered glioma tissues as tumor models. These models offer insights into the behavior of tumor cells within a three-dimensional environment and can facilitate the study of the interactions between tumor cells and their surrounding environment, thereby enabling effective investigations into glioblastoma cell migration.

#### ACKNOWLEDGEMENTS

The authors acknowledge the financial support from the National Institute of General Medical Sciences of the National Institutes of Health (7R01GM144417) and National Science Foundation (CMMI 2243771 and CMMI 2340016).

## REFERENCES

[1] Shafiee, A., and Atala, A., 2017, "Tissue Engineering: Toward a New Era of Medicine," *Annu. Rev. Med.*, **68**(1), pp. 29–40.

[2] Boyce, S. T., and Lalley, A. L., 2018, "Tissue Engineering of Skin and Regenerative Medicine for Wound Care," *Burns Trauma*, **6**.

[3] Vig, K., Chaudhari, A., Tripathi, S., Dixit, S., Sahu, R., Pillai, S., Dennis, V. A., and Singh, S. R., 2017, "Advances in Skin Regeneration Using Tissue Engineering," *Int. J. Mol. Sci.*, **18**(4), p. 789.

[4] Rijal, G., and Li, W., 2017, "A Versatile 3D Tissue Matrix Scaffold System for Tumor Modeling and Drug Screening," *Sci. Adv.*, **3**(9), p. e1700764.

[5] Smith, A. S. T., Macadangdang, J., Leung, W., Laflamme, M. A., and Kim, D.-H., 2017, "Human iPSC-Derived Cardiomyocytes and Tissue Engineering Strategies for Disease Modeling and Drug Screening," *Biotechnol. Adv.*, **35**(1), pp. 77–94.

[6] Roy, V., Magne, B., Vaillancourt-Audet, M., Blais, M., Chabaud, S., Grammond, E., Piquet, L., Fradette, J., Laverdière, I., Moulin, V. J., Landreville, S., Germain, L., Auger, F. A., Gros-Louis, F., and Bolduc, S., 2020, "Human Organ-Specific 3D Cancer Models Produced by the Stromal Self-Assembly Method of Tissue Engineering for the Study of Solid Tumors," *BioMed Res. Int.*, **2020**, p. e6051210.

[7] MacQueen, L. A., Sheehy, S. P., Chantre, C. O., Zimmerman, J. F., Pasqualini, F. S., Liu, X., Goss, J. A., Campbell, P. H., Gonzalez, G. M., Park, S.-J., Capulli, A. K., Ferrier, J. P., Kosar, T. F., Mahadevan, L., Pu, W. T., and Parker, K. K., 2018, "A Tissue-Engineered Scale Model of the Heart Ventricles," *Nat. Biomed. Eng.*, **2**(12), pp. 930–941.

[8] Beliveau, A., Thomas, G., Gong, J., Wen, Q., and Jain, A., 2016, "Aligned Nanotopography Promotes a Migratory State in Glioblastoma Multiforme Tumor Cells," *Sci. Rep.*, **6**(1), p. 26143.

[9] Jin, G., He, R., Sha, B., Li, W., Qing, H., Teng, R., and Xu, F., 2018, "Electrospun Three-Dimensional Aligned Nanofibrous Scaffolds for Tissue Engineering," *Mater. Sci. Eng. C*, **92**, pp. 995–1005.

[10] Liu, Y., Wang, S., and Zhang, R., 2017, "Composite Poly(Lactic Acid)/Chitosan Nanofibrous Scaffolds for Cardiac Tissue Engineering," *Int. J. Biol. Macromol.*, **103**, pp. 1130–1137.

[11] Rinoldi, C., Fallahi, A., Yazdi, I. K., Campos Paras, J., Kijeńska-Gawrońska, E., Trujillo-de Santiago, G., Tuoheti, A., Demarchi, D., Annabi, N., Khademhosseini, A., Swieszkowski, W., and Tamayol, A., 2019, "Mechanical and Biochemical Stimulation of 3D Multilayered Scaffolds for Tendon Tissue Engineering," *ACS Biomater. Sci. Eng.*, **5**(6), pp. 2953–2964.

[12] Damiati, L., Eales, M. G., Nobbs, A. H., Su, B., Tsimbouri, P. M., Salmeron-Sanchez, M., and Dalby, M. J., 2018, "Impact of Surface Topography and Coating on Osteogenesis and Bacterial Attachment on Titanium Implants," *J. Tissue Eng.*, **9**, p. 2041731418790694.

[13] Mozetic, P., Giannitelli, S. M., Gori, M., Trombetta, M., and Rainer, A., 2017, "Engineering Muscle Cell Alignment through 3D Bioprinting," *J. Biomed. Mater. Res. A*, **105**(9), pp. 2582–2588.

[14] Chen, C., Bai, X., Ding, Y., and Lee, I.-S., 2019, "Electrical Stimulation as a Novel Tool for Regulating Cell Behavior in Tissue Engineering," *Biomater. Res.*, **23**(1), p. 25.

[15] Pardo, A., Gómez-Florit, M., Barbosa, S., Taboada, P., Domingues, R. M. A., and Gomes, M. E., 2021, "Magnetic Nanocomposite Hydrogels for Tissue Engineering: Design Concepts and Remote Actuation Strategies to Control Cell Fate," *ACS Nano*, **15**(1), pp. 175–209.

[16] Brugger, M. S., Grundein, S., Doyle, A., Theogarajan, L., Wixforth, A., and Westerhausen, C., 2018, "Orchestrating Cells on a Chip: Employing Surface Acoustic Waves towards the Formation of Neural Networks," *Phys. Rev. E*, **98**(1), p. 012411.

[17] Cohen, S., Sazan, H., Kenigsberg, A., Schori, H., Piperno, S., Shpaisman, H., and Shefi, O., 2020, "Large-Scale Acoustic-Driven Neuronal Patterning and Directed Outgrowth," *Sci. Rep.*, **10**(1), p. 4932.

[18] Sripitukti, Y., Kasetsirikul, S., Ketpun, D., and Zhou, Y., 2019, "Cell Alignment and Accumulation Using Acoustic Nozzle for Bioprinting," *Sci. Rep.*, **9**(1), p. 17774.

[19] Naseer, S. M., Manbachi, A., Samandari, M., Walch, P., Gao, Y., Zhang, Y. S., Davoudi, F., Wang, W., Abrinia, K., Cooper, J. M., Khademhosseini, A., and Shin, S. R., 2017, "Surface Acoustic Waves Induced Micropatterning of Cells in Gelatin Methacryloyl (GelMA) Hydrogels," *Biofabrication*, **9**(1), p. 015020.

[20] Wang, J., Soto, F., Ma, P., Ahmed, R., Yang, H., Chen, S., Wang, J., Liu, C., Akin, D., Fu, K., Cao, X., Chen, P., Hsu, E.-C., Soh, H. T., Stoyanova, T., Wu, J. C., and Demirci, U., 2022, "Acoustic Fabrication of Living Cardiomyocyte-Based Hybrid Biorobots," *ACS Nano*, **16**(7), pp. 10219–10230.

[21] Armstrong, J. P. K., Puetzer, J. L., Serio, A., Guex, A. G., Kapnisi, M., Breant, A., Zong, Y., Assal, V., Skaalure, S. C., King, O., Murty, T., Meinert, C., Franklin, A. C., Bassindale, P. G., Nichols, M. K., Terracciano, C. M., Huttmacher, D. W., Drinkwater, B. W., Klein, T. J., Perriman, A. W., and Stevens, M. M., 2018, "Engineering Anisotropic Muscle Tissue Using Acoustic Cell Patterning," *Adv. Mater.*, **30**(43), p. 1802649.

[22] Tian, Z., Wang, Z., Zhang, P., Naquin, T. D., Mai, J., Wu, Y., Yang, S., Gu, Y., Bachman, H., and Liang, Y., 2020, "Generating Multifunctional Acoustic

Tweezers in Petri Dishes for Contactless, Precise Manipulation of Bioparticles,” *Sci. Adv.*, **6**(37), p. eabb0494.

[23] Yin, C., Jiang, X., Mann, S., Tian, L., and Drinkwater, B. W., 2023, “Acoustic Trapping: An Emerging Tool for Microfabrication Technology,” *Small*, **19**(26), p. 2207917.